Antiproton Flux, Antiproton-to-Proton Flux Ratio, and Properties of Elementary Particle Fluxes in Primary Cosmic Rays Measured with the Alpha Magnetic Spectrometer on the International Space Station

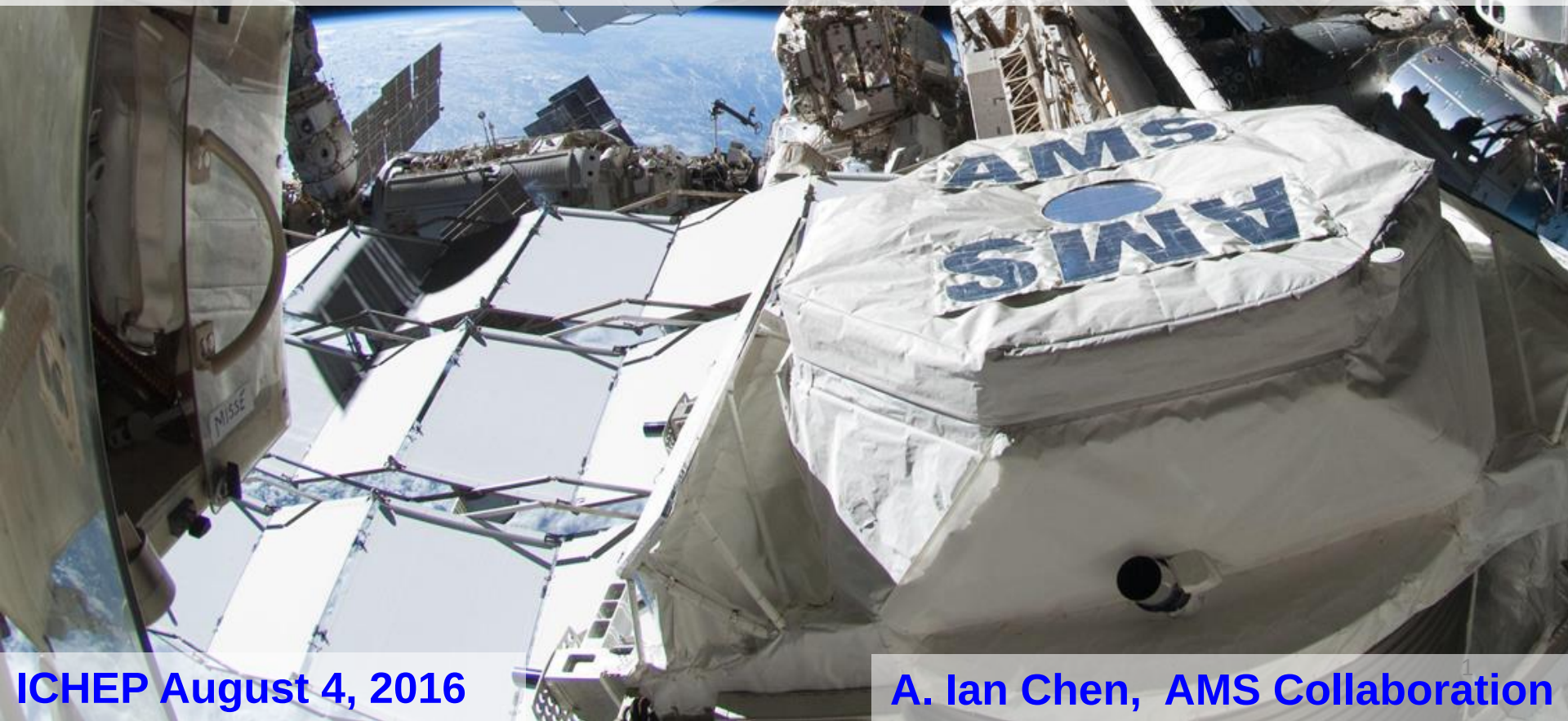

ICHEP August 4, 2016

A. Ian Chen, AMS Collaboration

Selection and Identification of $\bar{p}$ events from over 65 billion cosmic ray triggers uses all six of the AMS subdetectors

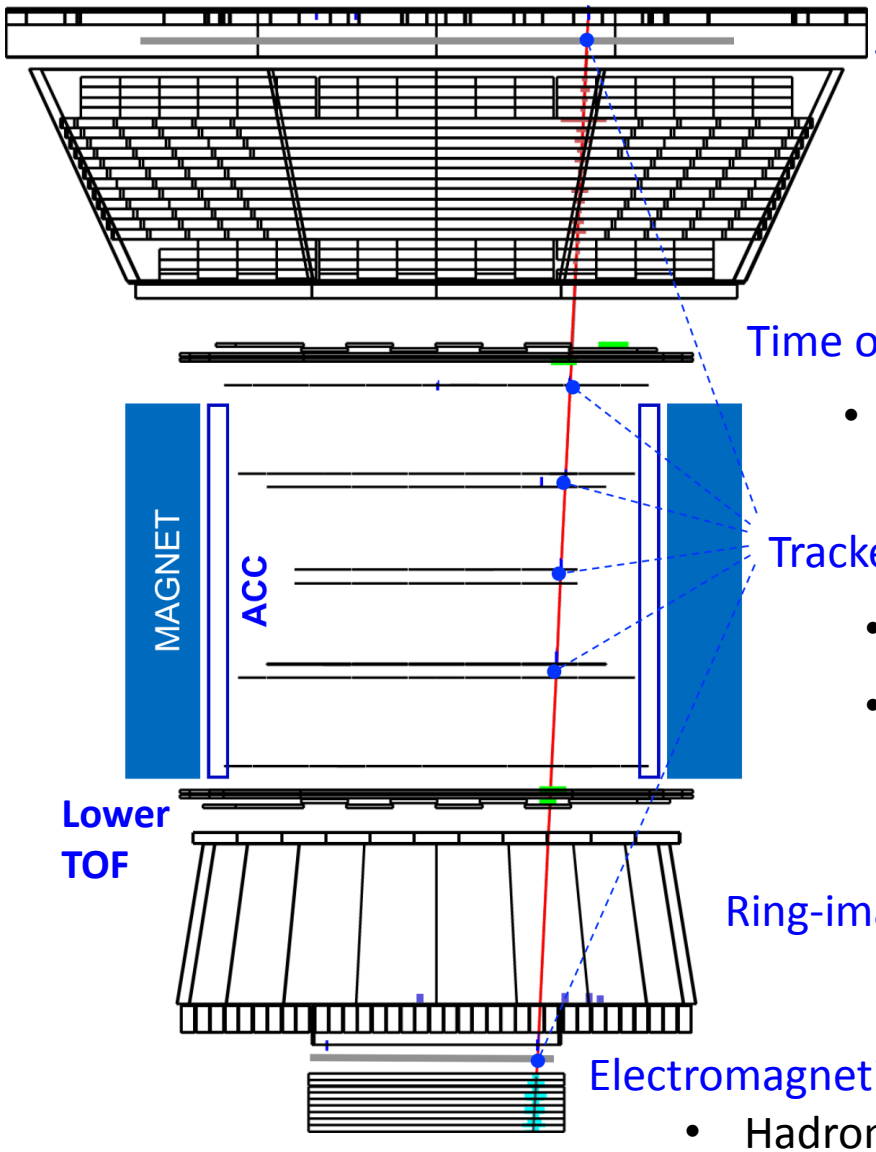

Transition Radiation Detector:

- At least 12 hits
- Separate $\bar{p}$ and p from e^- and e^+ using Λ_{TRD}

Time of Flight $\frac{\Delta\beta}{\beta} = 4\%$:

- Downgoing with $\beta > 0.3$

Tracker Maximum detectable rigidity 2 TV :

- Track quality, $\frac{\chi^2}{d.f.} < 10$
- $0.8 < |Q| < 1.2$

Ring-imaging Cherenkov detector $\frac{\Delta\beta}{\beta} = 0.1\%$

Electromagnetic Calorimeter 17 X_0 :

- Hadronic shower shape
- e^- sample selection

$R = -363$ GV antiproton

Selected events are further divided into positive and negative rigidity samples

Transition Radiation Detector discriminates electrons. Velocity measurements by TOF and RICH discriminate light mesons.

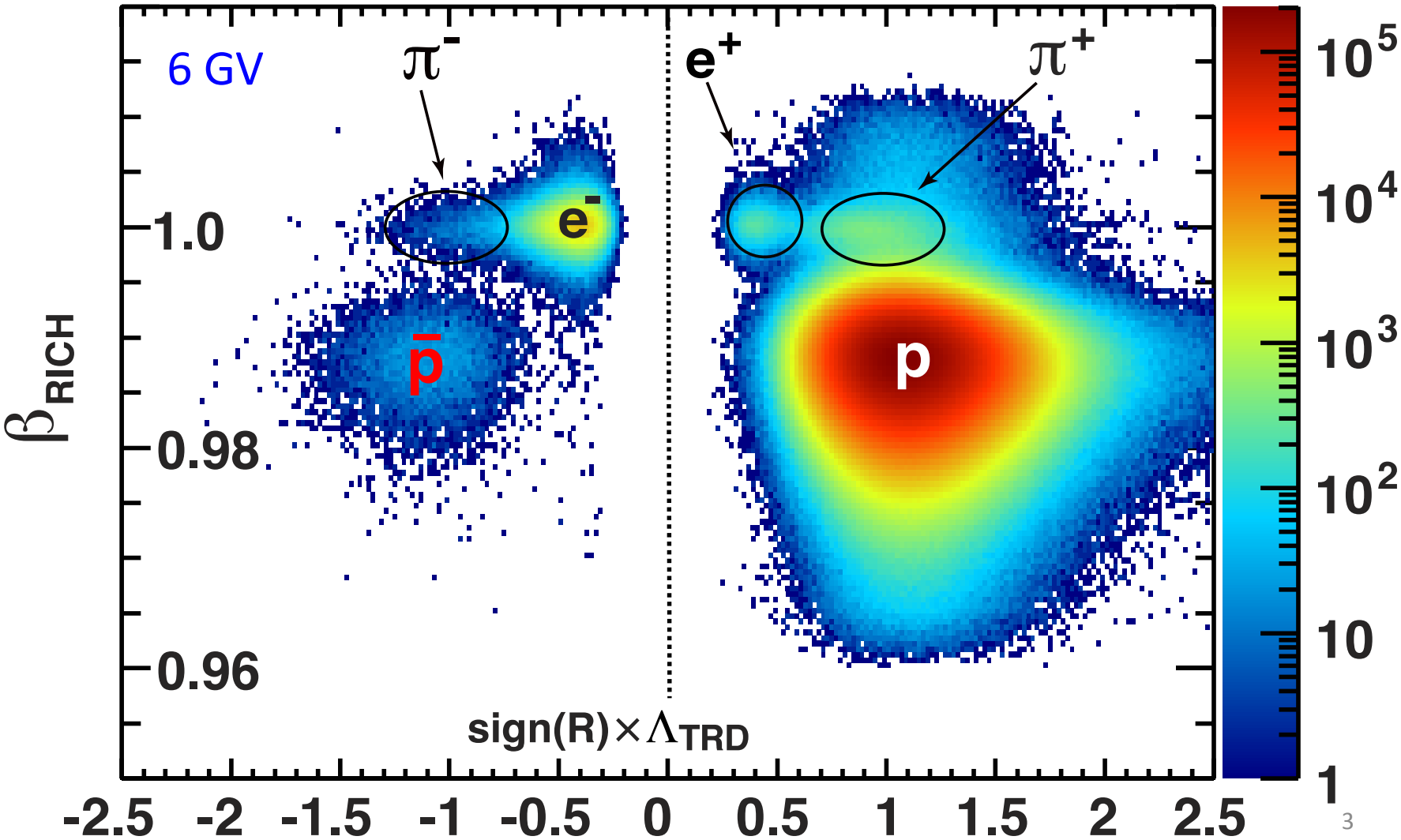

At high rigidities, charge confusion is the primary background for the negative sample

Protons contaminate the negative reconstructed rigidity sample due to finite tracker resolution and interactions. To identify these charge confusion protons, a charge confusion estimator, Λ_{CC}, is constructed using a boosted decision tree technique.

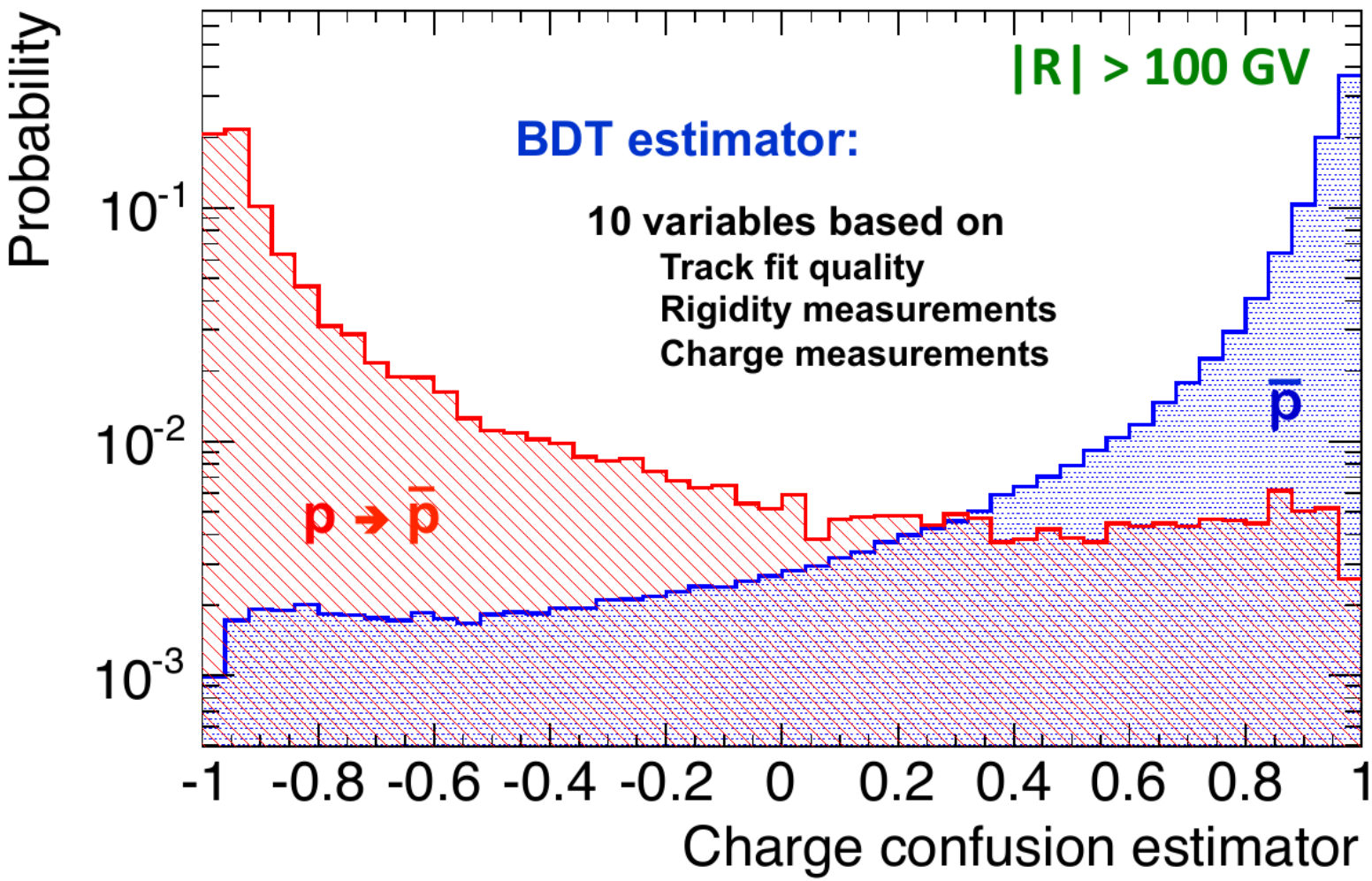

A two-dimensional fit along TRD and charge confusion classifiers determines the number of $\bar{p}$ events

- The template for $\bar{p}$ with correct charge-sign is defined by the high statistics p sample.
- The templates for e^- is based on Monte Carlo simulation, verified with ECAL.
- The charge confusion p are based on a Monte Carlo simulation, uncertainties included in systematic errors.

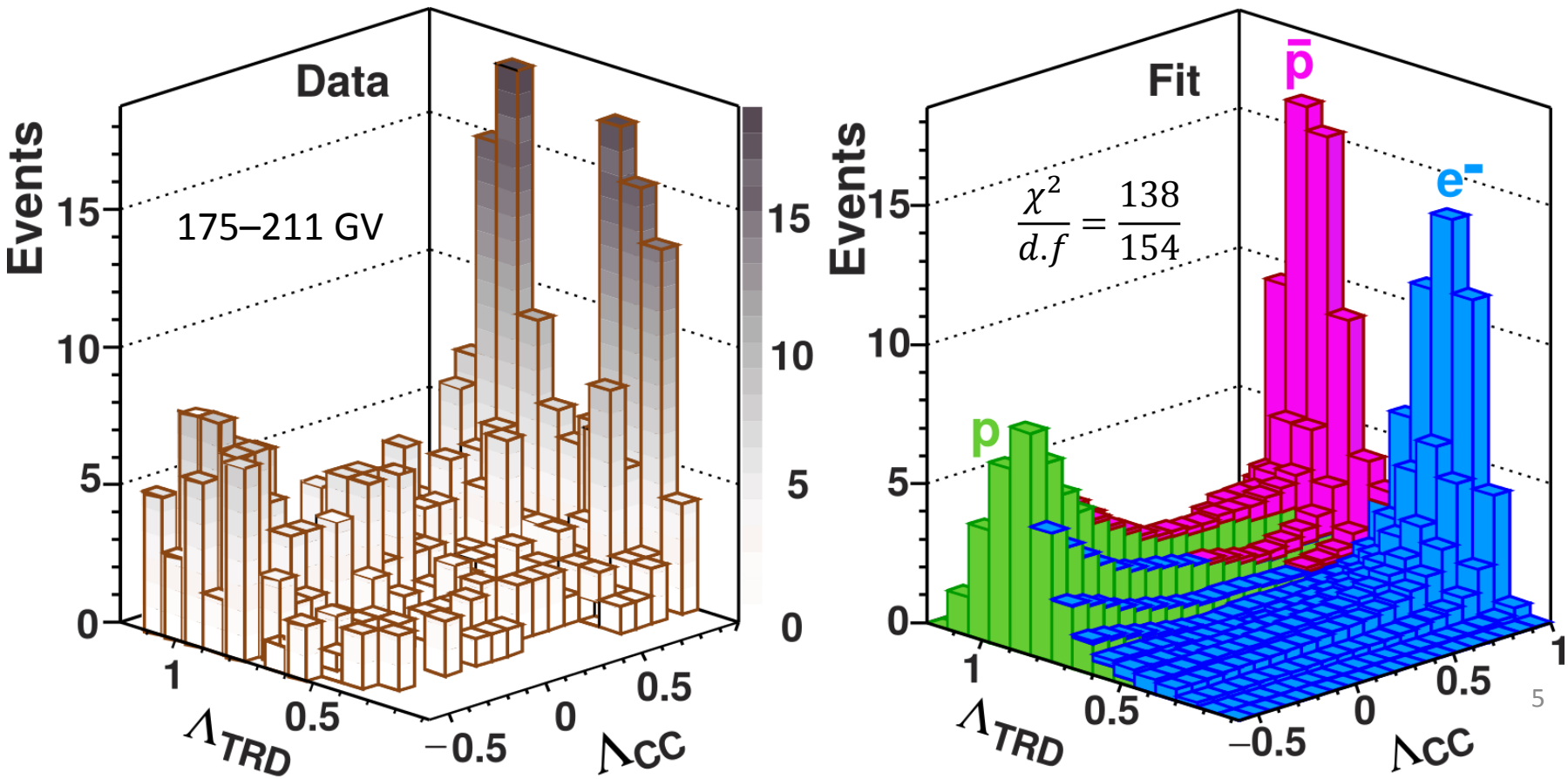

The $\bar{p}$ flux based on 3.49×10^5 events

Flux of $\bar{p}$
i = 57 bins
1–450 GV

$$\Phi_i^{\bar{p}}(R_i) = \frac{N_i^{\bar{p}}}{A_i^{\bar{p}} T_i \Delta R_i}$$

Events corrected for bin-to-bin migration

Rigidity bin

Effective acceptance

Exposure time

Bin width

There are four major sources of systematic error on the flux

1) Systematic errors on $N_i^{\bar{p}}$
   - Geomagnetic cutoff factor
   - Event selection
   - Template shape

2) Systematic errors on $A_i^{\bar{p}}$
   - Uncertainties in the inelastic cross-section
   - Bin-to-bin migration corrections on the effective acceptance

3) Systematic errors on absolute rigidity scale
   - Verified with e^- and e^+ data and E/p matching
   - ~1% at 450 GV

4) Systematic errors on absolute normalization of $A_i^{\bar{p}}$
   - Cancels in the flux ratio

1) Systematic errors on $N_i^{\bar{p}}$

Systematic errors from geomagnetic cutoff factor:

- ~1% at 1 GV and negligible above
- Verified by varying the safety factor applied to the cutoff value. The cutoff is calculated from backtracking the latest IGRF model.

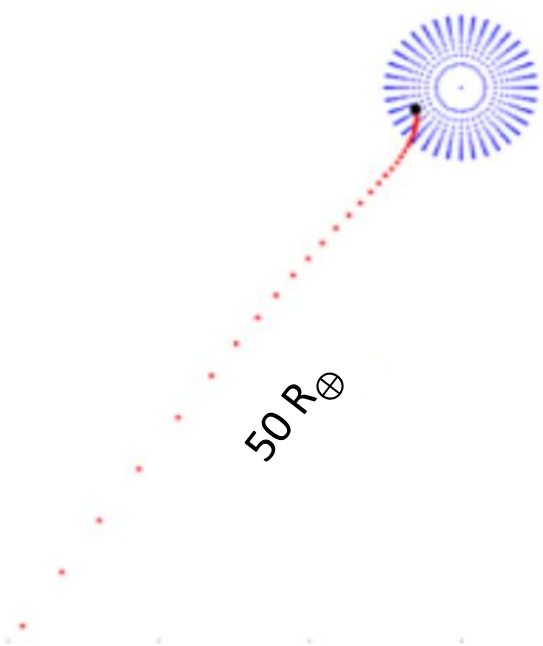

Systematic errors from event selection:

- 4% at 1 GV
- 0.5% at 10 GV
- 6% at 450 GV
- Stability in each bin tested over 1000 cut values. Varied requirements on track quality, ECAL shower shape, fit range, etc.

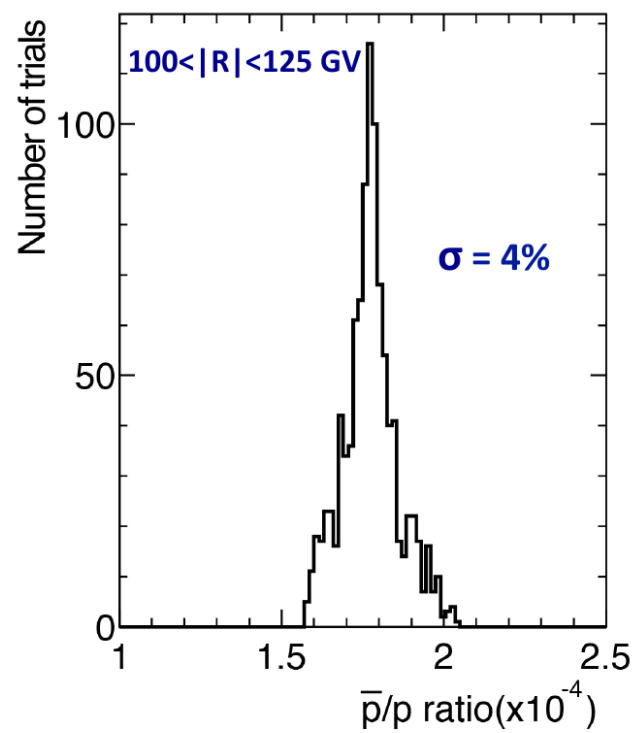

1) Systematic errors on $N_i^{\bar{p}}$: Template shape

- Template shape uncertainties are 12% at 450 GV decreasing to < 1% below 30 GV
- Rigidity resolution function is verified by 400 GV test beam
- Uncertainties from the proton flux in the TV region are accounted for by varying the spectral index within the accuracy of the p flux measurement
- A completely independent data-driven analysis based on a linear regression method for |R| > 30 GV is consistent with the template fit

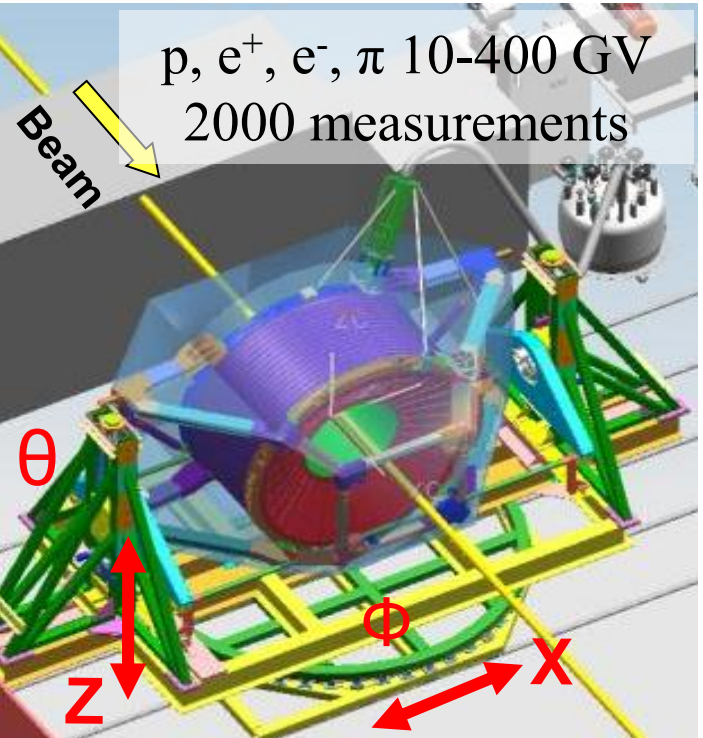

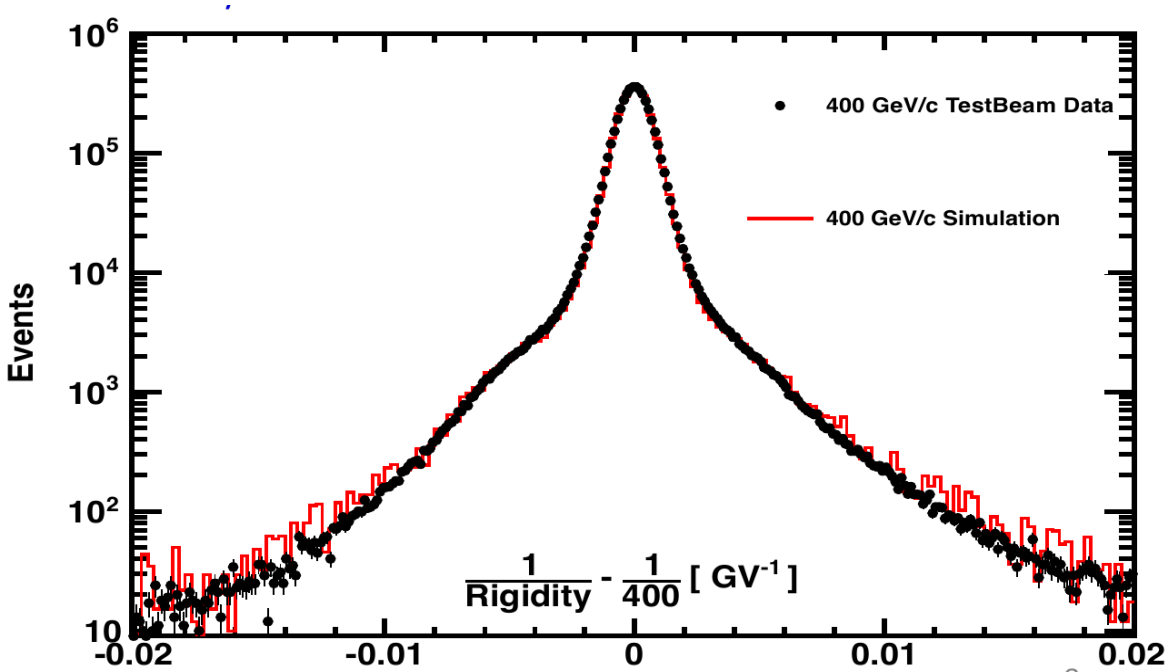

2) The systematic error on $A_i^{\bar{p}}$

The systematic error on $A_i^{\bar{p}}$ from cross-section uncertainties is found to be 4% at 1 GV and ~1% above 50 GV

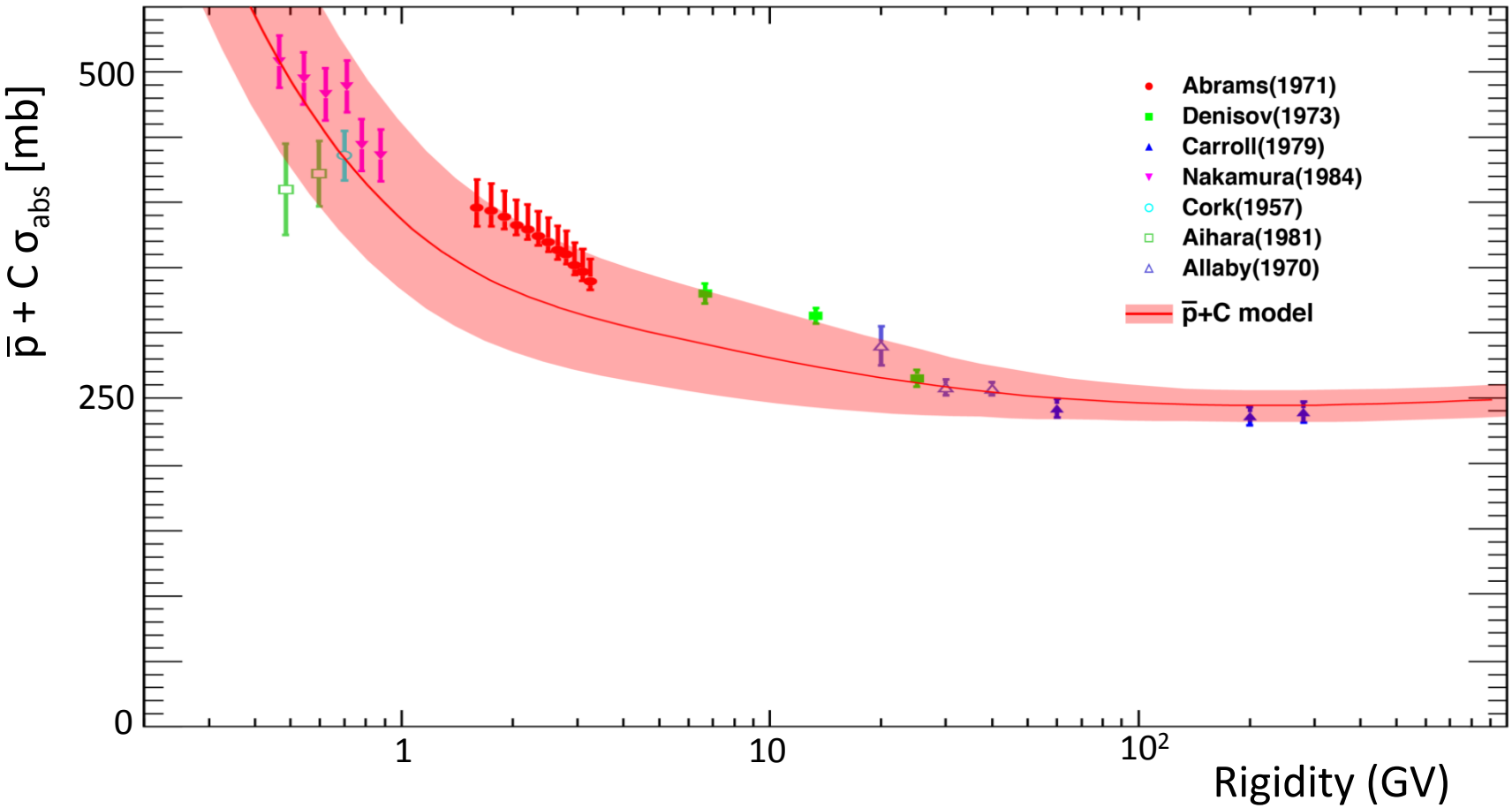

Inelastic cross−sections are varied in the GEANT 4.10.1 Monte Carlo simulation within the uncertainties

Errors on the $\bar{p}/p$ flux ratio

At 10 GV, uncertainties on the effective acceptance dominate. At high energies statistical errors are major contributions to the total error.

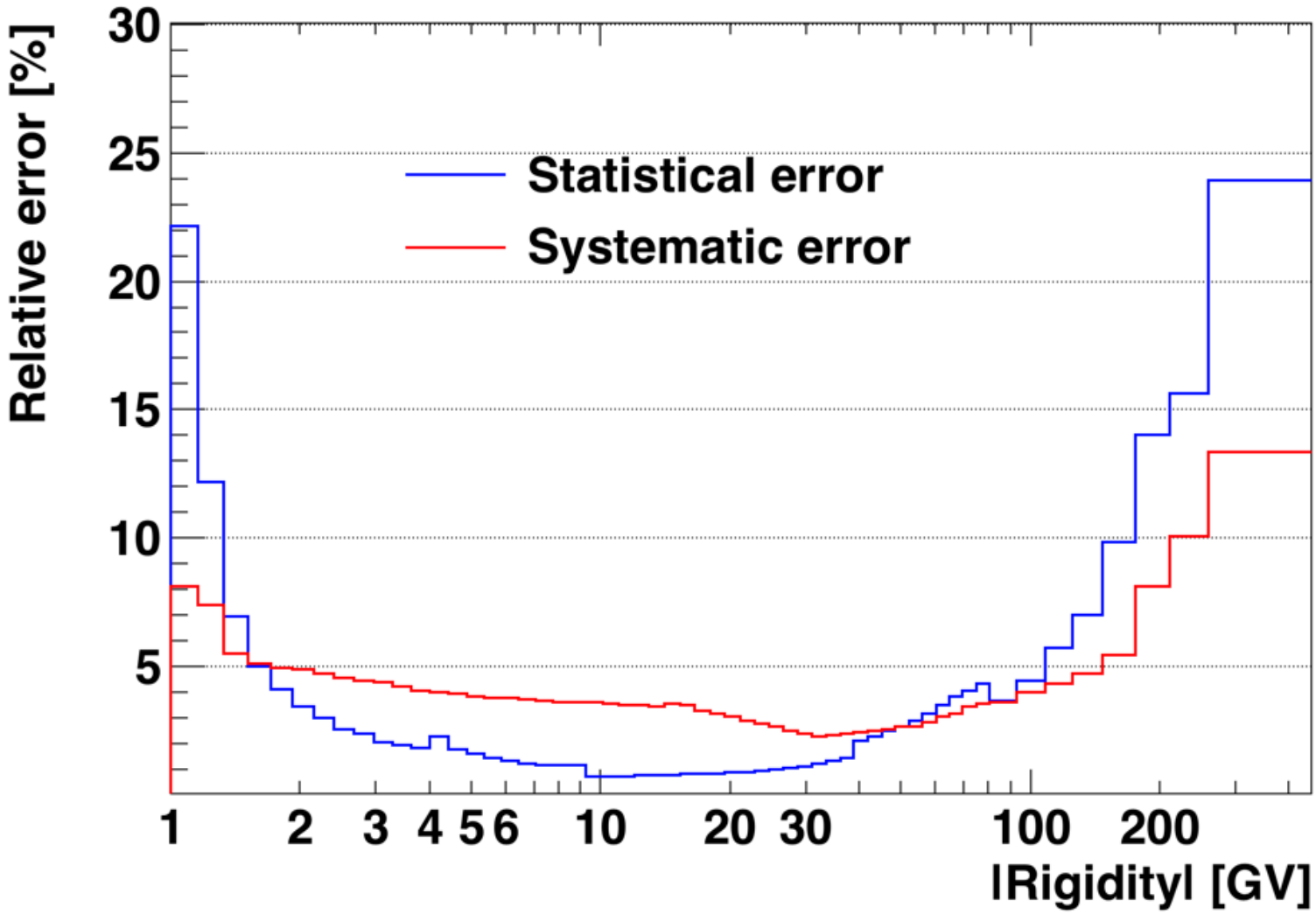

The $\bar{p}/p$ flux ratio

3.49×10^5 antiproton events and 2.42×10^9 proton events recorded from May 19, 2011 to May 26, 2015

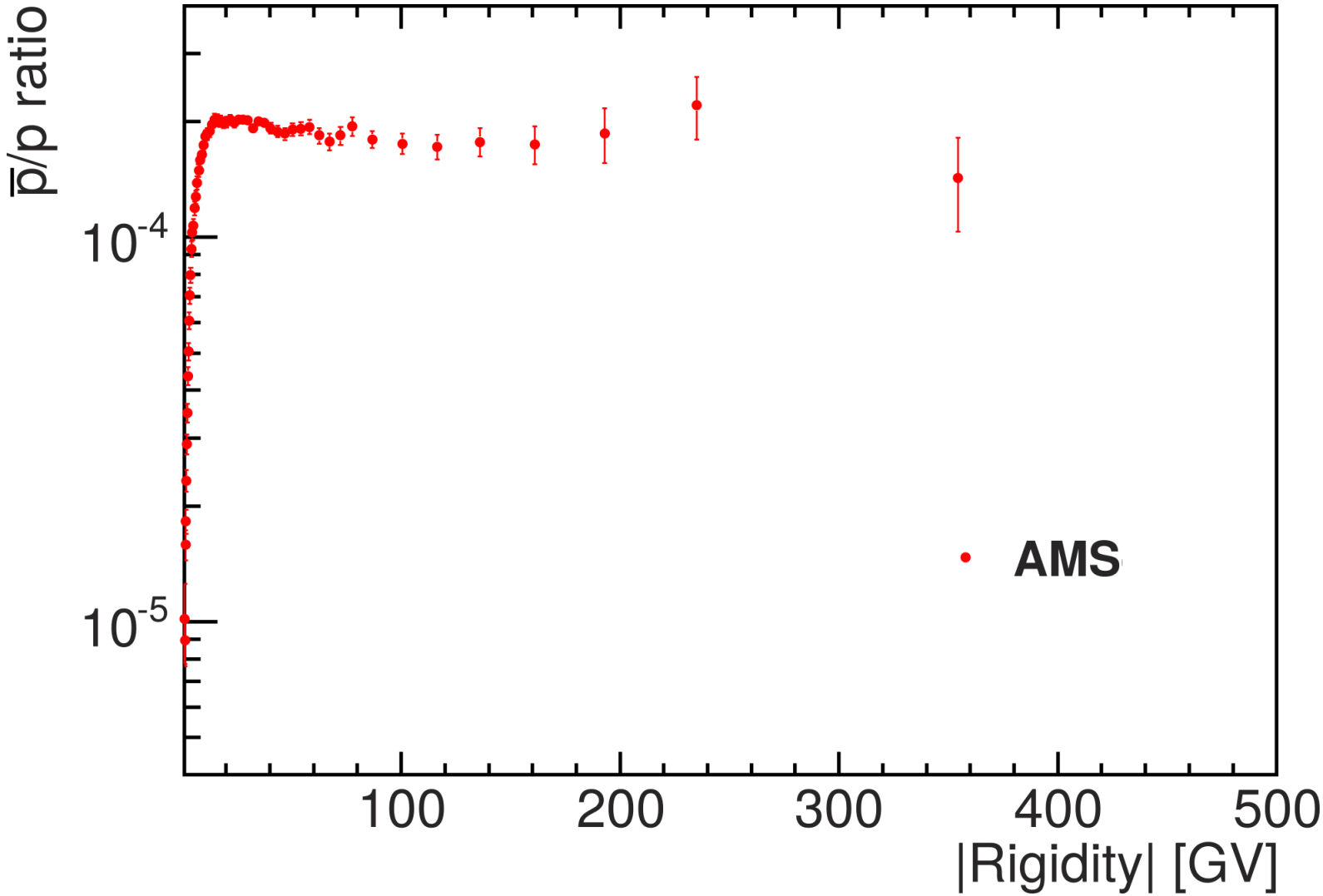

The $\bar{p}/p$ flux ratio

The measurement increases the precision and significantly extends the high rigidity range beyond previous observations.

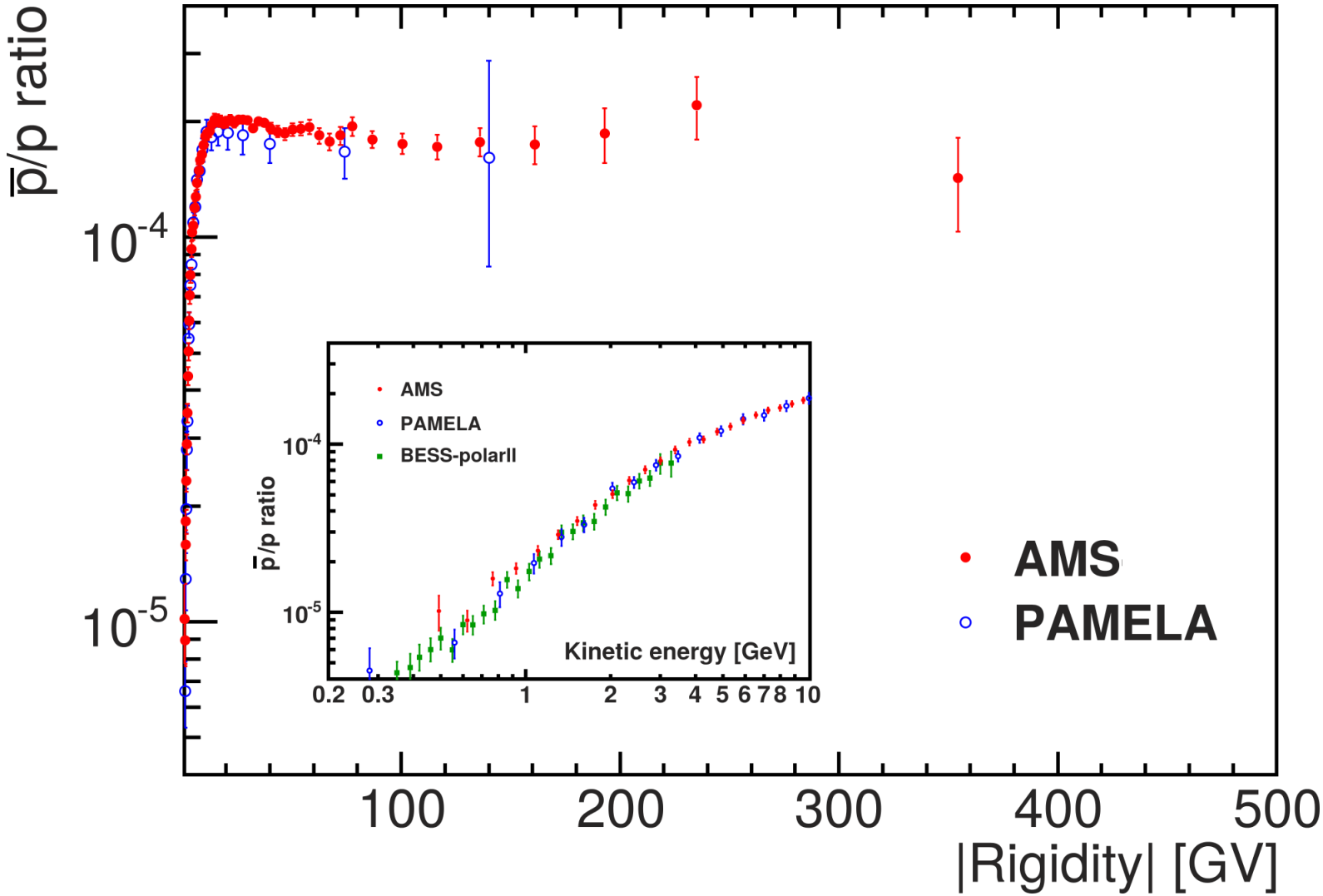

The spectral index for $\bar{p}$ compared with the p spectral index

Initially, the $\bar{p}$ spectral index decreases more rapidly.

For 60 GV < |R| < 400 GV the spectral indices are consistent.

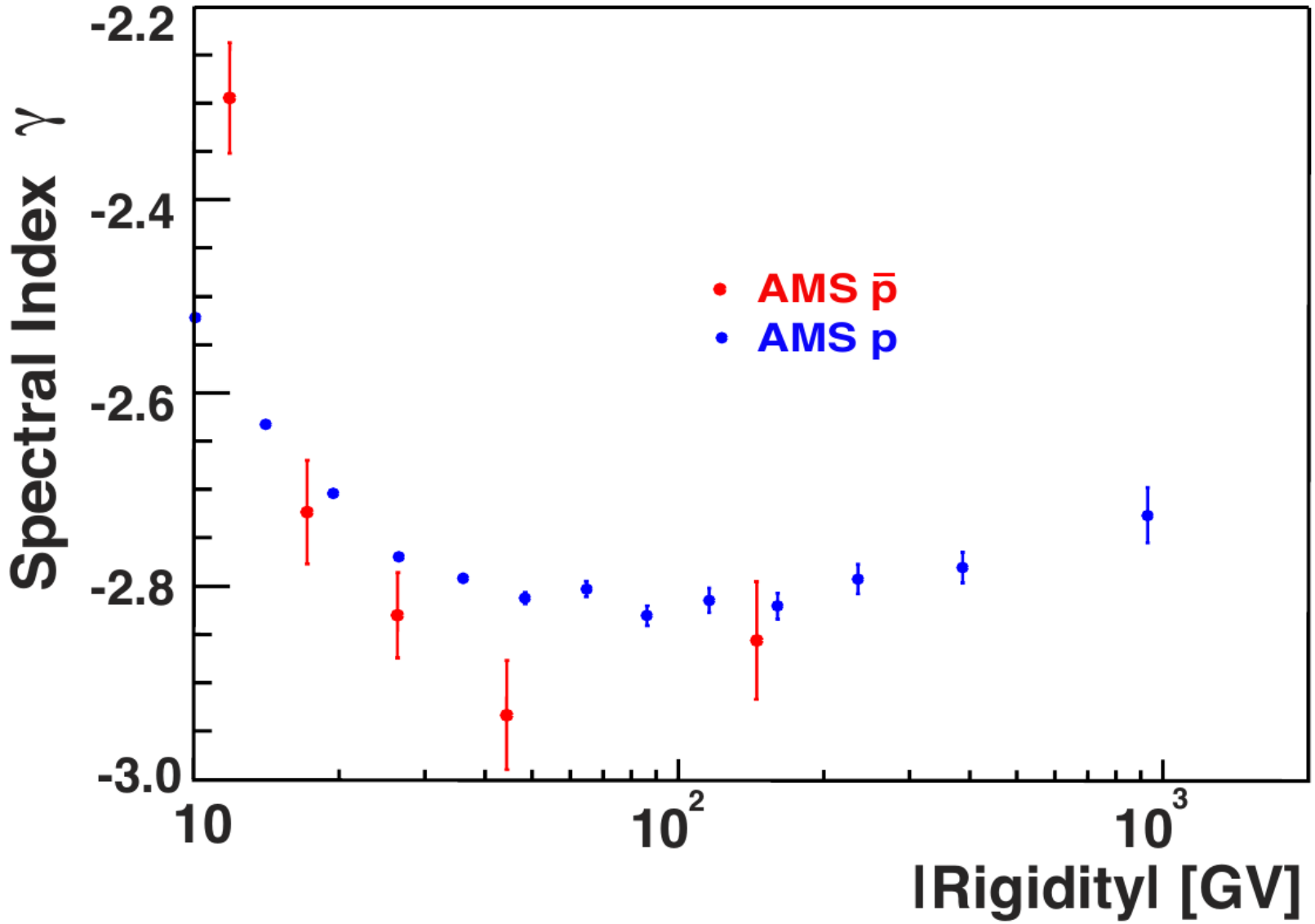

The place where the constant behavior begins is found to be 60.3 GV

An interval is split in two sections and fit by constants. The first interval where the constants are consistent at 90% c.l. defines the lowest limit.

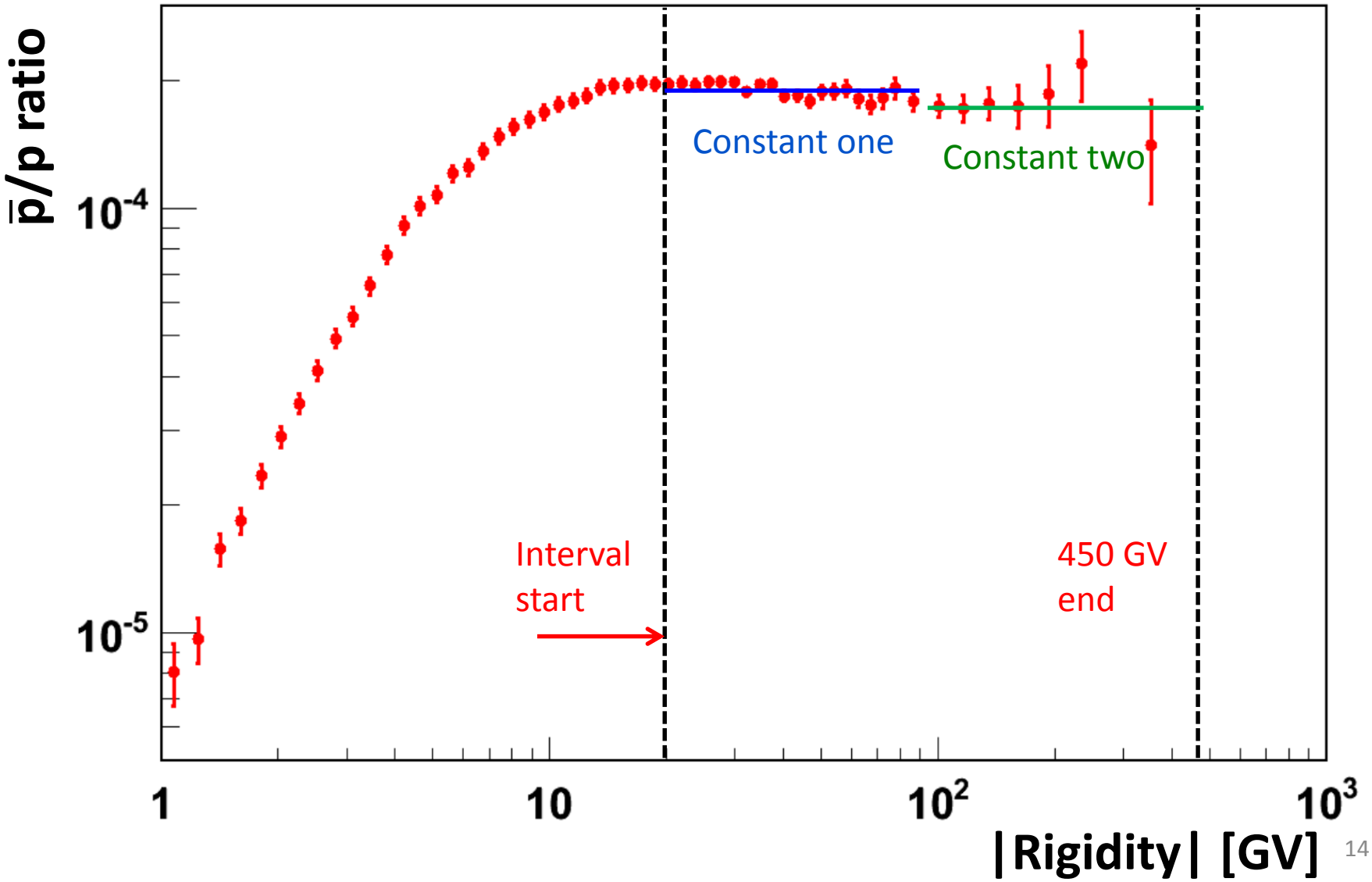

Elementary particle fluxes in primary cosmic rays

Spectrum of elementary particles e^+, $\bar{p}$, and p have identical energy dependence above 60 GV, but e^- does not.

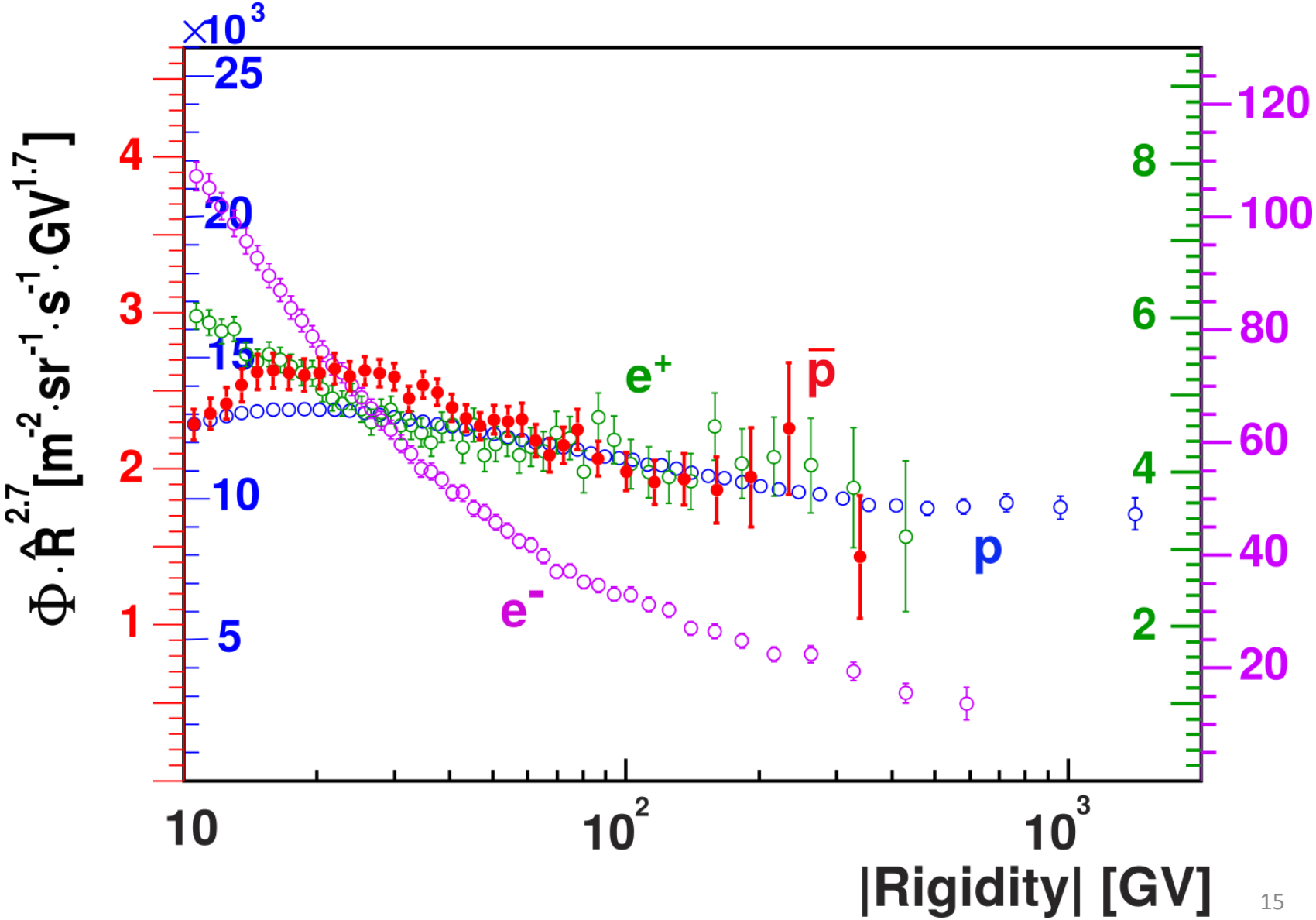

Flat behavior with linear fits

The ratios $\Phi^{\bar{p}}/\Phi^{p}$, $\Phi^{\bar{p}}/\Phi^{e^+}$, and Φ^{p}/Φ^{e^+} show no rigidity dependence. This was not expected.

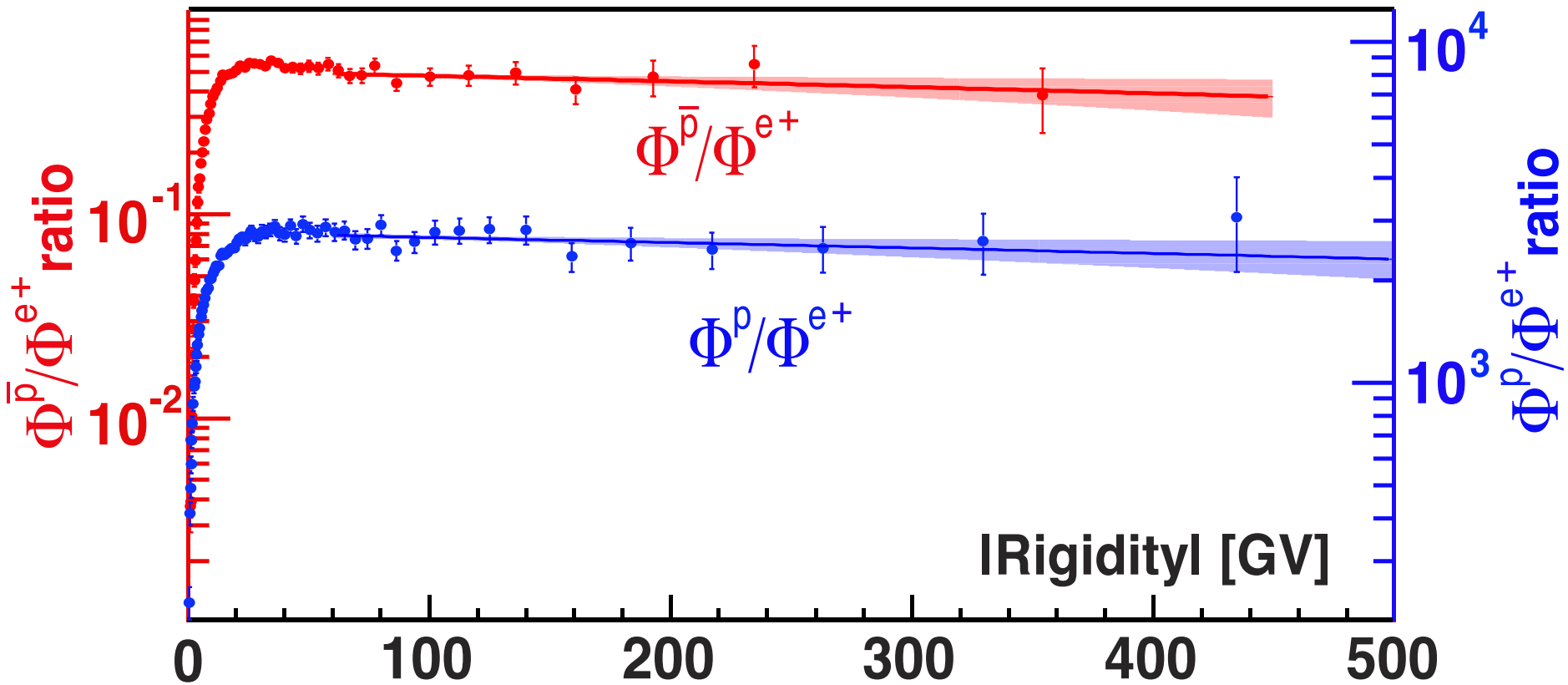

Rigidity dependent behaviour in e⁻ ratios

Unlike the other combinations, $\Phi^{\bar{p}}/\Phi^{e^-}$ and Φ^{p}/Φ^{e^-} show rigidity dependence. This contrast in behavior was not predicted before AMS.

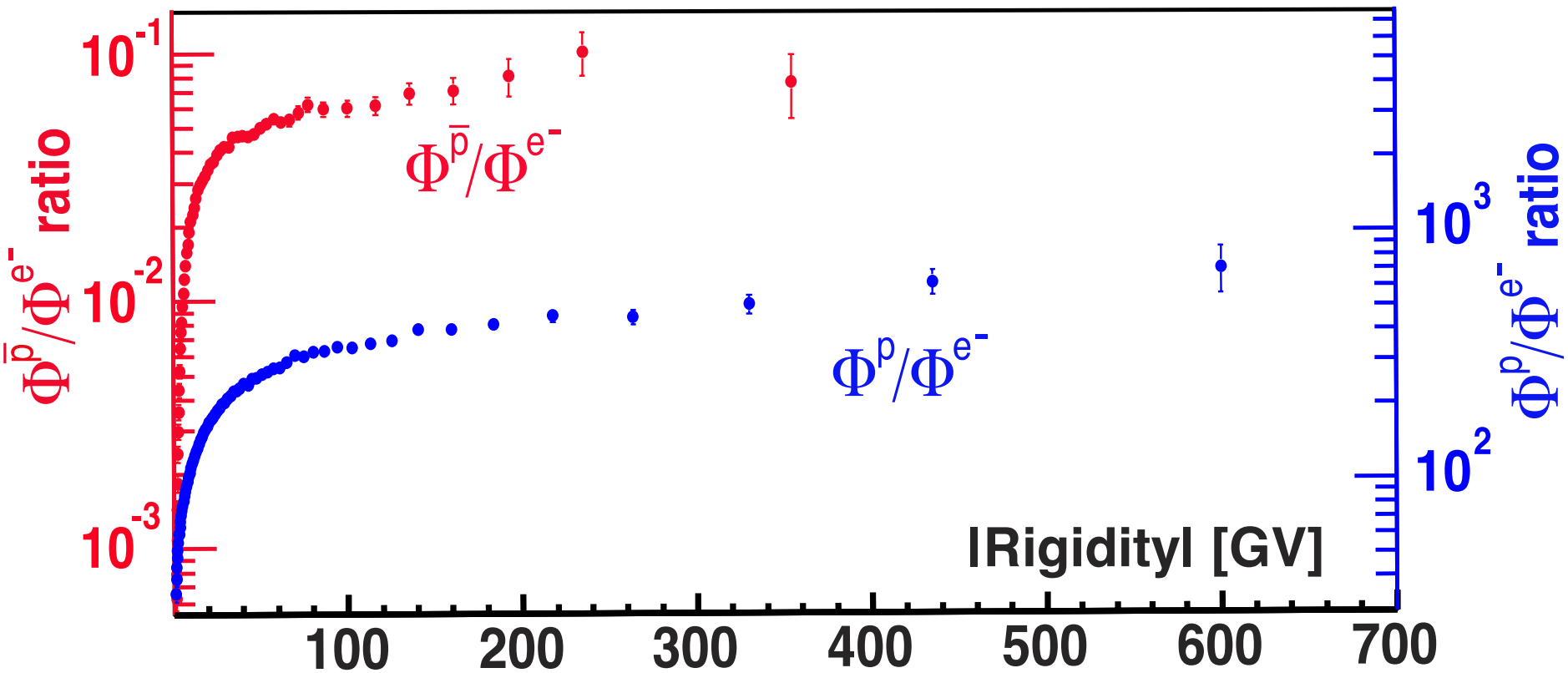

AMS has simultaneously measured all the charged elementary particle cosmic ray fluxes and flux ratios

The behavior of these fluxes and ratios are new observations of the properties of elementary particles in the cosmos.